ON THE IDENTIFICATION OF NORMAL MODES OF OSCILLATION FROM OBSERVATIONS OF THE SOLAR PERIPHERY

D.O. Gough, Institute of Astronomy and Department of Applied Mathematics and Theoretical Physics, University of Cambridge, UK and Joint Institute for Laboratory Astrophysics, Boulder, Colorado, USA
J. Latour, Observatoires du Pic-du-Midi et de Toulouse and Cray Research France, Paris, France

Keywords: Helioseismology, Legendre functions, solar oscillations

ABSTRACT
The decomposition of solar oscillations into their constituent normal modes requires a knowledge of both the spatial and temporal variation of the perturbation to the Sun's surface. The task can be especially difficult when only limited spatial information is available. Observations of the limb-darkening function, for example, are probably sensitive to too large a number of modes to permit most of the modes to be identified in a power spectrum of measurements at only a few points on the limb, unless the results are combined with other data. In this paper we consider a procedure by which the contributions from quite small groups of modes to spatially well resolved data obtained at any instant can be extracted from the remaining modes. Combining these results with frequency information then permits the modes to be identified, at least if their frequencies are low enough to ensure that modes of high degree do not contribute substantially to the signal.

I INTRODUCTION

Observations of the solar limb-darkening profile have been used in investigations of dynamical oscillations and solar diameter variations. Several instruments have been developed for sampling the time evolution of a measurable property of the limb-darkening function (Bos & Hill, 1983; Rösch & Yerle, 1983; Stebbins, 1984). We report here on a procedure applicable to observations of this kind that might lead to the identification of normal modes of oscillation of low and

intermediate degree. Mode identification is a necessary step in the process of extracting from the observations useful diagnostics of the solar interior. Then more stringent bounds on the internal density distribution and the internal motion might be found.

Identification of the modes is likely to be easier in regions of the temporal frequency spectrum where the modes are sparsely distributed. This is the region of the longer-period p modes, which have low order and low degree (see Figure 1). Of the p modes, these are the most sensitive to the structure of the deep solar interior. At present there is little information about these modes, but there is hope that future limb-darkening observations will be successful in measuring them.

Departures from spherical symmetry aside, the spatial structure of a normal mode is separable into a spherical-harmonic dependence on the horizontal coordinates and a function of radius. We choose a spherical polar coordinate system about the rotation axis, and make the simplifying assumption that the axis is perpendicular to the line of sight. Moreover we ignore any deviation from axisymmetry in the equilibrium state, such as might be produced by an intense magnetic field and which would produce complicated fine structure in the frequency spectrum.

Spherical harmonics form a complete orthogonal basis on the sphere with respect to which one can make a unique decompositon of any well-behaved function. From the orthogonality of this basis on the entire sphere, it follows that we cannot uniquely determine the expansion coefficients if we know the function on only a fraction of the sphere. Such limited spatial information is unavoidable when observing the Sun from Earth, or any other single location, and the limitations are especially severe when information is available only from the solar limb. Therefore from data obtained at only one instant in time there is bound to be some ambiguity in identifying modes. However, to a considerable extent we can compensate the lack of geometrial information with temporal information, by analysing the distribution of the frequencies of the modes.

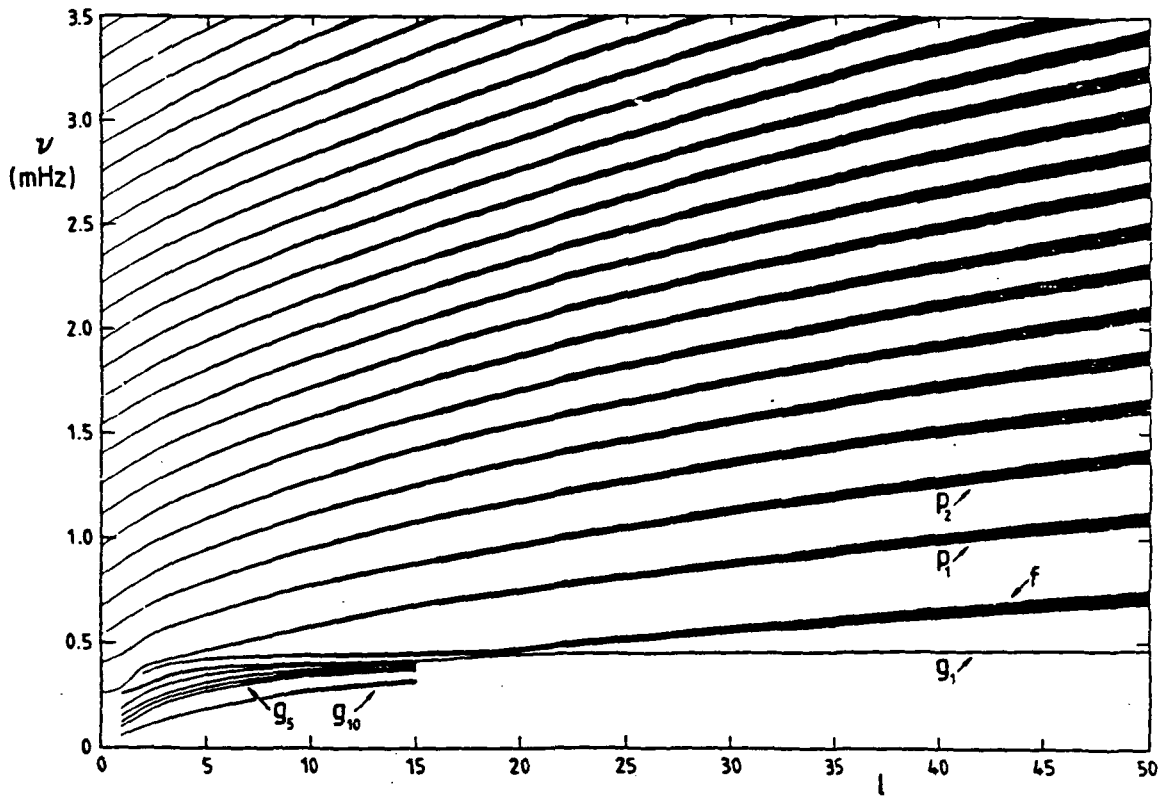

Figure 1. Cyclic frequencies ν of normal modes of oscillation of Christensen-Dalsgaard's (1982) Model 1 of the present Sun. Each set of modes of like order n is plotted against degree ℓ and joined by a continuous line; the centres of the lines pass through the frequencies of the axisymmetric modes, and the thickness of the lines (except that for g_1) represents the extent of rotational splitting under the assumption that the Sun is rotating rigidly at the surface equatorial rate. Only a few g modes are included, to avoid cluttering the diagram. The g_1 line marks the upper frequency limit of any axisymmetric g mode at the appropriate value of ℓ.

In this paper we develop an optimal mode separation procedure that combines data obtained from observations around the solar limb at any instant in such a way as to minimize the influence of modes other than that under investigation. We are not always able to obtain a combination that is expected to be dominated by only a single mode. However, it is possible to reduce the number of contributing modes severely. Provided the degrees ℓ of the modes that can be detected is adequately limited, either by virtue of the frequency range being studied or as a result of a decline in instrumental sensitivity at high

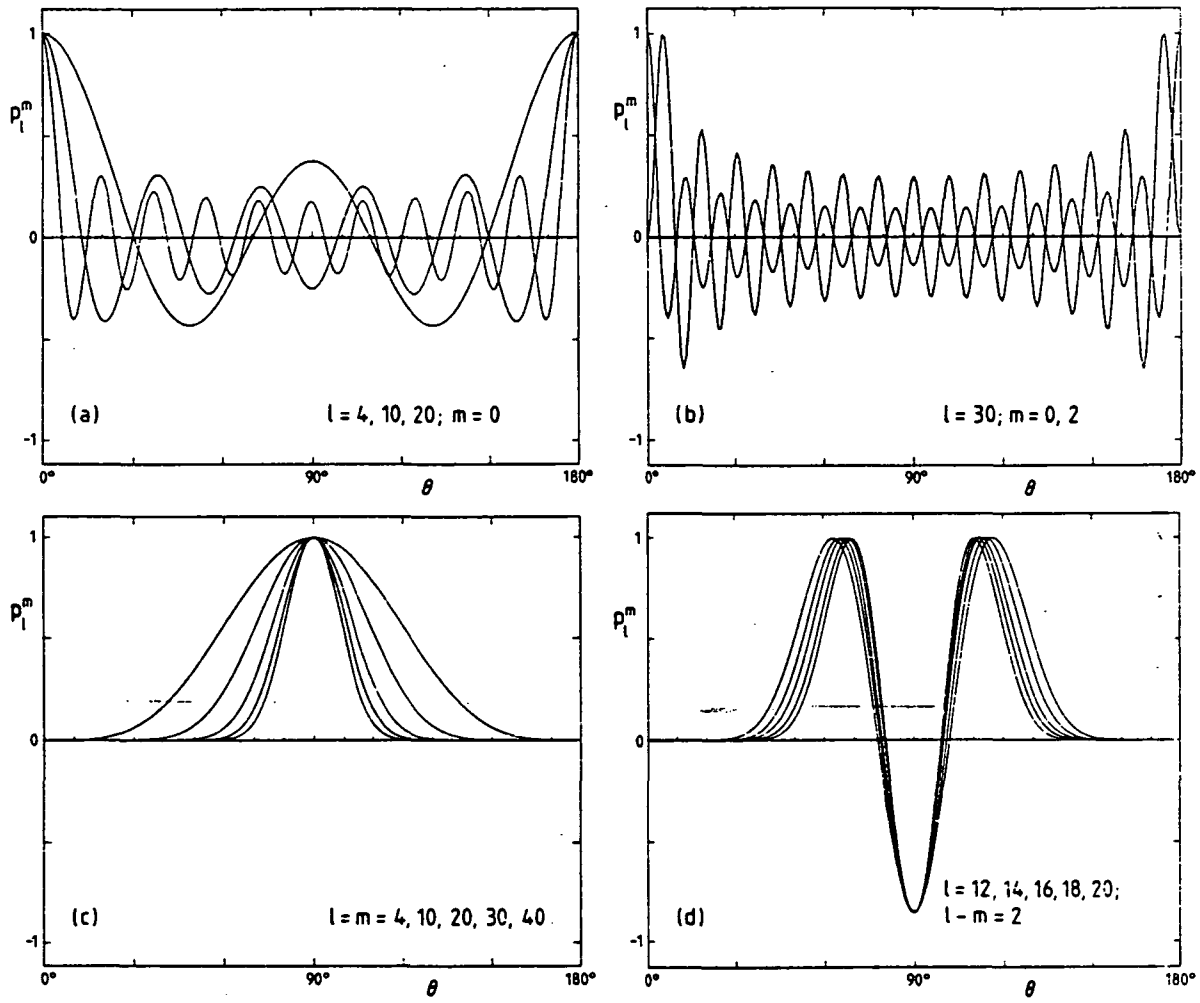

Figure 2. A selection of associated Legendre functions, normalized to a maximum magnitude of unity and plotted against θ. The values of ℓ and m are stated in each box; the individual curves can be identified by the number of zeros in (a) and (b) or by the degree of equatorial concentration in (c) and (d).

ℓ, the temporal information can then be used to identify the modes. An extension of this study to two-dimensional observations of the solar disk will be presented by Christensen-Dalsgaard (1984).

II GEOMETRICAL STRUCTURE OF ASSOCIATED LEGENDRE FUNCTIONS

The latitudinal dependence of spherical harmonics is given by the associated Legendre function $P_\ell^m(\cos\theta)$, where θ is colatitude and ℓ and m are respectively the degree and azimuthal order of the mode. With our

assumption that the observer is in the equatorial plane, the emplitude of the perturbation to the limb-darkening function associated with a normal mode is proportional to P_ℓ^m. Therefore it is convenient first to point out a few simple geometrical properties of the Legendre functions that will help in understanding the results. In Figure 2 we display several examples of these functions, scaled so that they each have a maximum magnitude of unity.

When $m = 0$ (Figure 2a) P_ℓ^m is a Legendre polynomial, whose magnitude is larger near the poles than the equator. The latitudinal variation increases with ℓ, so that at large ℓ the mode would be most easily visible near the poles. With low m and $\ell >> m$ (Figure 2b), functions P_ℓ^m with the same ℓ, corresponding to modes with almost the same frequency, have essentially the same spatial structure everywhere but near the poles, and separating them by observation would be extremely difficult unless one can obtain very high spatial resolution close to the poles.

When $\ell = m$ (Figure 2c) a very different situation occurs: then the functional form of P_ℓ^m reduces to $\sin^m \theta$, yielding, when m is large, a substantial amplitude only very close to the equator. Equatorial concentration occurs also when $0 \neq \ell - m << \ell$, as is evident in Figure 2d, the half-width of the region of substantial amplitude being approximately

$$\theta_o = \cos^{-1} \{ m [\ell (\ell+1)]^{-\frac{1}{2}} \} . \qquad (1)$$

Figure 2d shows quite clearly that the differences between modes with $\ell-m << \ell$ having the same value of $\ell-m$ are hardly discernable, since their nodes and antinodes are in similar locations. Thus we foresee the kind of limitations any identification procedure must suffer.

III THE LIMB SIGNAL

The signal extracted from the limb-darkening function at a given point on the periphery defined by $\mu_i = \cos \theta_i$ can be written:

$$\tilde{s}(\mu_i,t) = \sum_k A_k\, Q_k(\mu_i)\, \cos(\omega_k t - pm\phi - \epsilon_k) + \text{noise}, \qquad (2)$$

where k stands for the set of integers (p,n,ℓ,m) identifying each mode of oscillation, ϕ is the azimuthal angle and ϵ_k are constants. The integer n is the order of the mode and p can take the values ± 1. Our convention is to regard $m > 0$. Thus $p = +1$ signifies prograde modes and $p = -1$ signifies retrograde modes. We suppose that we know, at a given instant t, $4(N-1)$ measurements of $\tilde{s}$ distributed around the entire limb of the Sun. In the specific examples we study, we always take the data to be distributed uniformly in θ.

The functions Q_k are proportional to associated Legendre functions. We take $Q_k \equiv \alpha_{\ell m} P_\ell^m$, choosing the scaling factors $\alpha_{\ell m}$ to make the spherical harmonics $S_\ell^m(\theta,\phi) \equiv Q_k(\cos\theta)\begin{matrix}\sin\\ \cos\end{matrix} m\phi$ have unit rms over the sphere. Thus

$$\int_0^\pi [Q_k(\cos\theta)]^2 \sin\theta\, d\theta = \frac{4}{1+\delta_{m0}}, \qquad (3)$$

where δ_{ij} is the Kronecker delta.

The quantities A_k are the products of the physical amplitudes of the modes and the instrumental sensitivity to the associated spherical harmonics. The latter depends on the precise way in which the measurements are performed; it declines with increasing ℓ and m, at least when ℓ and m are large. According to Hill (1978), for example, the efficiency of some of his measurements is greater than 50 per cent only when $\ell \lesssim 50$, and for convenience we assume uniform sensitivity for all modes with $\ell \lesssim \ell_m$ for some ℓ_m, and ignore modes with $\ell > \ell_m$. If temporal filtering is performed one also encounters an upper bound to ℓ at frequencies above the g-mode limit, as is evident in Figure 1. Thus the series (2) contains a finite number of terms, and the factors A_k may be considered to represent the physical amplitudes of the modes. Most of our computations have been performed with $\ell_m = 40$, since the details in the illustrations would be difficult to discern if ℓ_m were greater.

Our normalization (3) implies that p modes with different low or intermediate degrees and azimuthal orders but with similar frequencies and the same amplitudes A_k have similar kinetic energies, as has been pointed out for the case of five-minute oscillations (Christensen-Dalsgaard and Gough, 1982). Thus for the p modes under consideration here we anticipate the statistical expectation of A_k to be independent of ℓ and m, as it appears to be for the five-minute modes. This is what one would expect if the modes are excited stochastically by convection.

Symmetry considerations permit us to separate modes with odd and even values of m by adding or subtracting signals on the east and west sides of the limb($\phi = \pm\pi/2$) at the same latitude. Modes with even and odd $\ell - m$ can be similarly separated, by adding or subtracting signals from the north and south. We can thus reduce by a factor of four the number of modes that need be considered simultaneously. The problem that remains is equivalent to separating a given component k_c from a set of N signals

$$s(\mu_i) = \sum_k A_k Q_k(\mu_i) + \sigma_i \qquad (4)$$

with m and ℓ even (say), where σ_i is the noise at μ_i and $0 \leq \mu_i \leq 1$. The sum in Equation (4) contains $K = (\ell_m+2)(\ell_m+4)/8$ terms.

IV PROJECTIONS ONTO ASSOCIATED LEGENDRE FUNCTIONS

In an attempt to separate the mode designated by some particular value k_c of k, we first ignore the noise and seek a set of coefficients $a_i(k_c)$ such that in the linear combination

$$S_{k_c} \equiv \sum_i a_i(k_c)\, s(\mu_i) \simeq \sum_k \{ \sum_i a_i(k_c) Q_k(\mu_i) \} A_k \equiv \sum_k W_k(k_c) A_k \qquad (5)$$

the quantity W_k is large when $k = k_c$ and small otherwise. If we were to succeed, then

$$S_{k_c} = W_{k_c} A_{k_c}, \qquad (6)$$

and we would have achieved our goal.

Before embarking on our optimal separation procedure we first investigate the extent to which a mode is isolated when the signal is projected onto the associated Legendre function corresponding to the mode in question. This, of course, is the procedure one would certainly

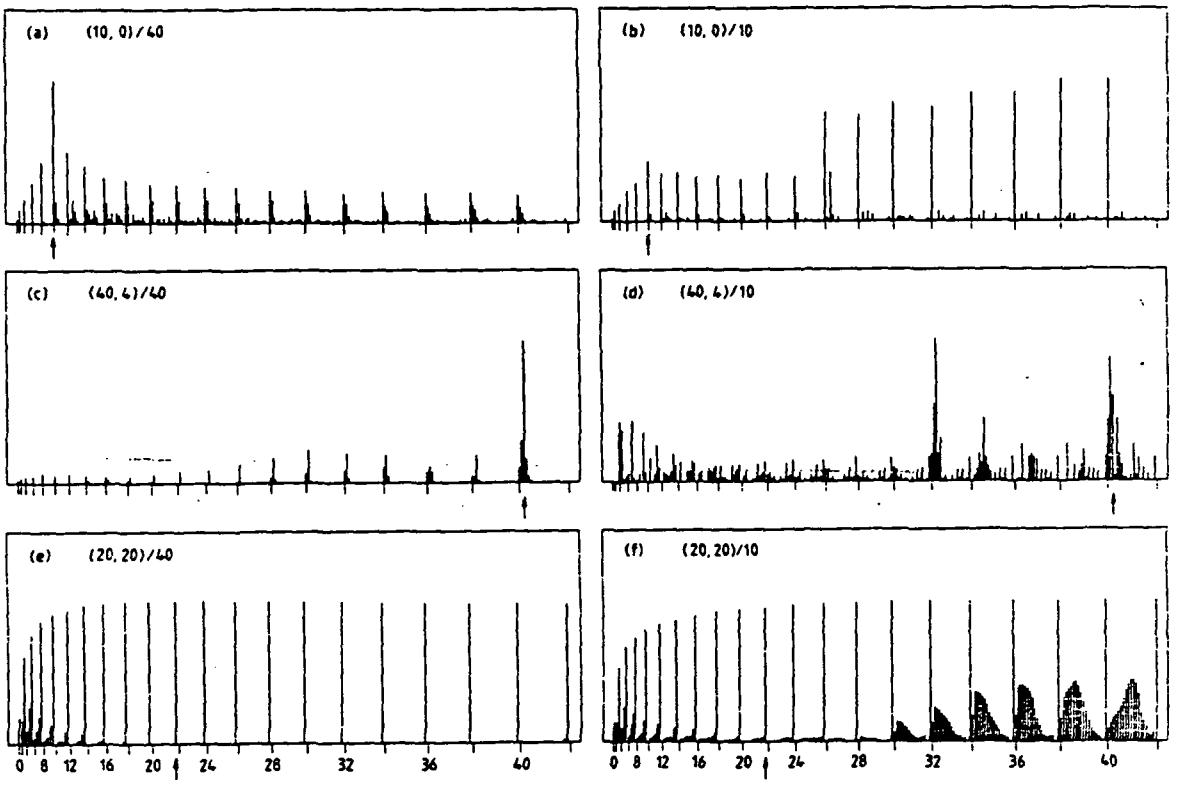

Figure 3.2 Bar chart representing $W_k^2(k_c)$. In this and subsequent figures, W_k is plotted against $\ell(\ell+2)/8 + m$ on a linear scale. The ticks on the abscissa are drawn where m = 0, and the labels refer to the values of ℓ. Thus each diagram is somewhat like a power spectrum of the combination S_{k_c} of data, plotted on a distorted frequency scale, and including only the prograde modes (p = +1) of like order n, all having the same amplitude. [In most cases the distortion of the frequency scale can be thought of as simply removing part of the frequency axis, but for low-order modes of high degree it can also entail separating the fine structure due to rotational splitting of modes with consecutive even values of ℓ.] In all the examples illustrated, the combinations include only modes with even degree ℓ and azimuthal order m. The degree ℓ_c and azimuthal order m_c (corresponding to k_c) of the mode that it is hoped to isolate, and the number N of observation points in a complete quadrant, are indicated in each box using the notation $(\ell_c, m_c)/N$. The position of that mode on the abscissa is shown by the arrow. In this figure the factors W_k were computed by projecting the signal onto the appropriate associated Legendre function, as described in the text.

have adopted were the functions Q_k to have been orthogonal. Thus we set $a_i(k_c) = Q_{k_c}(\nu_i)$ and evaluate W_k from Equation (5). We report in Section V that in many cases this simple operation is essentially as good as our optimization procedure.

A selection of results is illustrated in Figure 3. In this and the subsequent figures, W_k^2 is plotted in a bar chart as a function of $\ell(\ell+2)/8 + m$. Thus each chart resembles a power spectrum, of a set of only prograde modes of like order, plotted on a distorted frequency scale. (Note that any real spectrum would also contain the retrograde modes, and would be a superposition of the spectra of modes of all orders.)

In the three examples with N = 40, which represent combinations of data taken from 156 equally spaced points around the solar limb, W_{k_c} is no smaller than the other values of W_k, though only in case (c) is it more than twice as great as any other. As one might have anticipated from Figure 2b, the greatest contamination in Figure 3c comes from modes with the same degree and neighbouring azimuthal orders. In Figure 3a, where ℓ is not so large, contamination comes mainly from the other modes with the same value of m. Recall that when $\ell-m \ll \ell$ the associated Legendre functions with like $\ell-m$ are quite similar (see Figures 2c and 2d); consequently in Figure 3e one sees substantial contributions from nearly all the modes with like $\ell-m$.

Figures 3b, 3d and 3f have the same values of k_c as Figures 3a, 3c and 3e, but result from only 36 data points. Now the sampling is insufficient to resolve the structures of the modes adequately. In no case does the largest value of W_k correspond to the mode onto which the signal was projected.

We have so far confined our discussion to the extremes $m \ll \ell$ and $\ell-m \ll \ell$. An intermediate case ($\ell = 10$, $m = 4$) is illustrated in Figure 4. This mode does not have very fine structure, and appears to be adequately resolved when N = 15; the corresponding diagram for N = 40 is not shown, but it is almost indistinguishable from Figure 5c. There has been some success in producing a relatively high value of W_k for this mode, though the values for ($\ell = 8$, $m = 2$) and ($\ell = 12$, $m = 6$), are

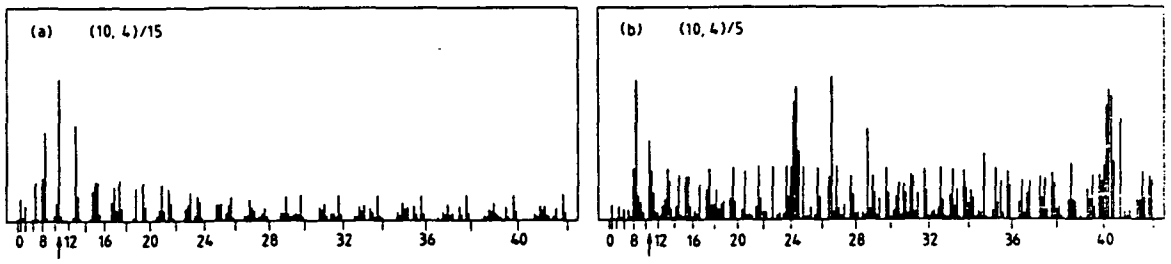

Figure 4. An example illustrating how isolation procedures fail when spatial resolution is inadequate.

high too. When only 16 data points are used, however, the situation is quite different, as is evident in figure 4b. That is hardly surprising, since a mode with $\ell-m = 6$ has 12 nodes around the limb, and cannot possibly be resolved by sampling at only 16 points.

V AN OPTIMAL MODE ISOLATION PROCEDURE

One might expect to improve the degree of isolation of a mode by choosing the coefficients a_i such as to optimize the extent to which $W_{k_c}^2$ exceeds the other values of W_k^2. The problem resembles that posed by Backus and Gilbert (1970) in their discussion of the resolving power of geophysical data. The following analysis, which takes cognisance of the inevitable errors in the data, is derived from that work.

We choose the coefficients a_i by minimizing for some value of λ the quantity

$$D(k_c) \equiv \sum_k J\,(k-k_c)\, W_k^{\,2}\,(k_c) + \lambda \sum_i \sum_j a_i E_{ij} a_j \qquad (7)$$

subject to the constraint

$$I \equiv \sum_k W_k^{\,2} = 1, \qquad (8)$$

where E_{ij} is the covariance matrix of the errors σ_i. The function J is chosen to be zero when $k = k_c$, and large for $k \neq k_c$. From numerical experiments we have found that the outcome of the mode separation procedure is insensitive to details of the shape of J. All the results we present here were obtained with

$$J = \begin{matrix} 0, \text{ if } k=k_c \\ 1, \text{ if } k\neq k_c. \end{matrix} \tag{9}$$

The presence of the double sum in the expression (7) for D reduces the influence of σ_i on S_{k_c} at the expense of increasing the contamination with undesired modes.

The problem of minimizing D under the constraint (8) is equivalent to the unconstrained minimization of

$$\Delta = I^{-1}D. \tag{10}$$

The Euler equations are

$$\sum_j (F_{ij} - \Delta G_{ij})a_j = 0, \tag{11}$$

where

$$F_{ij} = F_{ji} = \sum_k J Q_k(\mu_i) Q_k(\mu_j) + \lambda E_{ij}, \tag{12}$$

$$G_{ij} = G_{ji} = \sum_k Q_k(\mu_i) Q_k(\mu_j). \tag{13}$$

The desired coefficients a_i are the components of the eigenvector associated with the minimum eigenvalue $\Delta(k_c)$ of equation (11). From them we can compute the vector $W_k(k_c)$, and see whether it has the property we sought.

VI RESULTS

The method we have just outlined can be applied to any part of the freqency spectrum, but the success in isolating a small number of modes is bound to be the greatest in the range of the low-order p modes, where the upper bound ℓ_m to ℓ is relatively small (see Figure 1). From the $(\ell_m+2)(\ell_m+4)/8$ possible choices of k_c in this range we have extracted a few typical results. These are illustrated in Figures 5 and 6. They are all computed with $E_{ij} = \delta_{ij}$ and $\lambda = 1$.

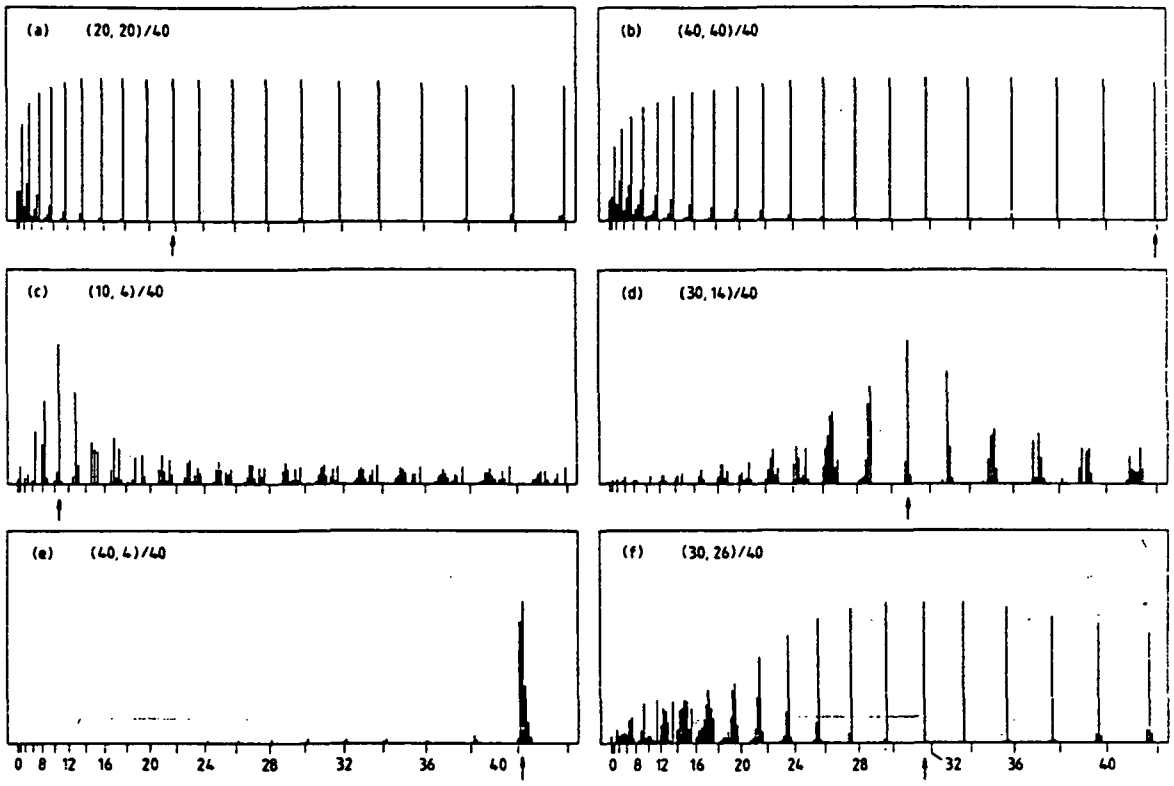

Figure 5. A selection of charts indicating W_k^2 computed by the optimal procedure described in section V of the text, using 40 observation points in a complete quadrant.

Results for sectoral modes ($m = \ell$) with $\ell_c = 20$ and $\ell_c = 40$ are shown in Figures 5a and 5b. They were obtained assuming measurements to have been made at 156 points around the limb and combined to yield 40 data points equally spaced in θ between 0 and $\pi/2$ containing signal from only those modes with even ℓ and m. The diagrams are quite similar, and reflect the fact that we cannot distinguish between the sectoral modes. However, we can extract the entire set of sectoral modes from the total signal, and efficiently suppress all other modes. This is because only the sectoral modes have a large amplitude very near the equator (Figure 2c). It is somewhat harder to isolate modes with small nonzero $\ell - m$ (see Figure 5f). Only at large ℓ are the shapes of the functions P_ℓ^m very similar (Figure 2d) when $\ell - m$ is fixed. Thus there is a tendency to have contamination particularly from low-degree modes. For intermediate $\ell - m$ (e.g. Figures 5c and 5d) the results are more complicated.

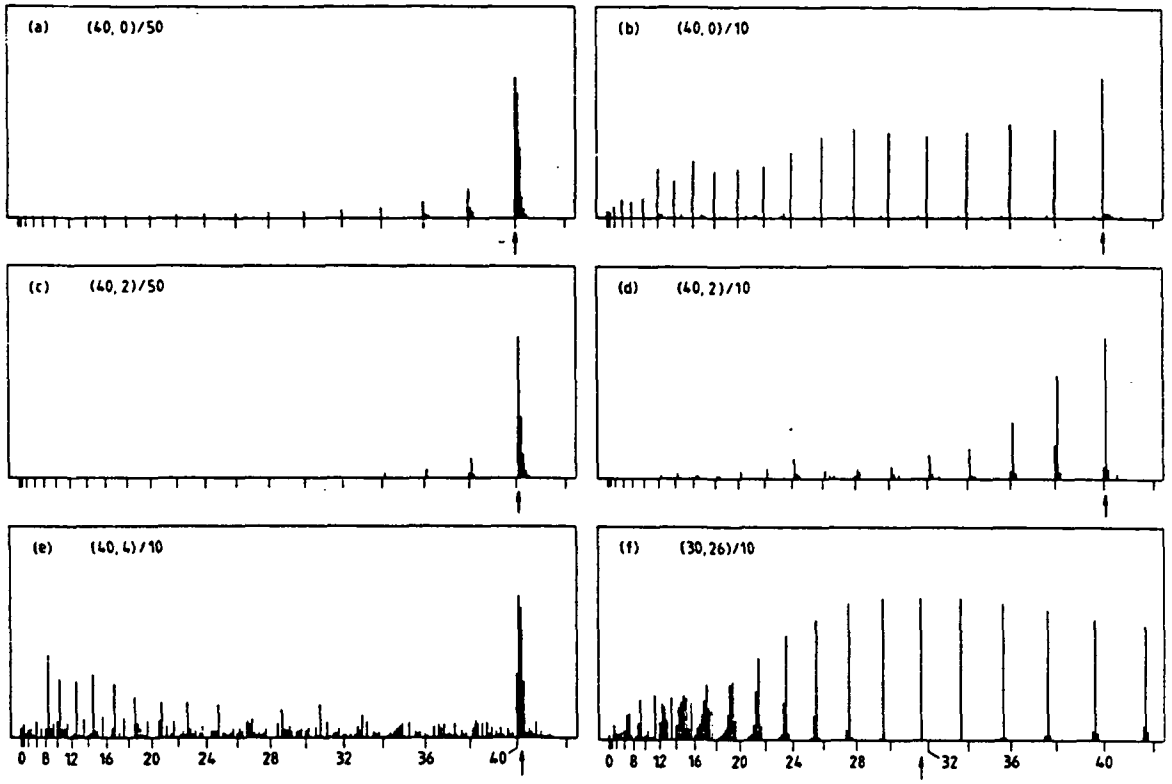

Figure 6. A selection of charts computed by the optimal procedure of section V, which, together with Figures 5c and 5f, indicate the importance of spatial resolution when trying to isolate different kinds of modes.

The case of low m and large ℓ, especially $\ell = \ell_m$, is peculiar. Since $\ell - m$ is now close to ℓ_m, the number of zeros of P_ℓ^m is quite rare in the whole set of modes. Therefore high spatial resolution will ensure a very good selection of such a mode (Figure 5e), limited only by the close similarity in shape for two successive values of m (see Figure 2b). When $\ell = \ell_m$ (= 40), the isolation procedure is therefore very efficient, keeping essentially only three or four modes out of 1681.

The values of the coefficients $a_i(k_c)$, considered as a function of the angular coordinate θ_i, are often quite similar to the particular associated Legendre function $P_\ell^m(\cos\theta_i)$ one tries to isolate. Consequently the results of the optimal isolation procedure do not differ markedly from the more straightforward projection onto the Legendre functions. Indeed, for high-degree sectoral modes the differences are barely discernible (cf. Figures 3e and 5a). In that particular case the coefficients a_i have large values only near the

equator, and it would be more efficient to perform the observations with a variable spatial resolution, having a finer distribution of observation points close to the equator. It does not matter that modes with moderate and large ℓ-m would then be less effectively removed in this case, because they have lesser amplitudes in the equatorial regions where the major contribution to the combination S_{k_c} is provided.

Experiments have also been performed with low resolution (N = 10) and the same values of k_c. On the whole there is some deterioration in the results (Figure 6), though in some cases contamination is not as severe as was found when $a_i(k_c)$ was set to $Q_{k_c}(\mu_i)$. Generally the deterioration is most pronounced for modes that cease to be adequately resolved at the lower value of N. In view of these results, it seems desirable that future observations of the limb-darkening function be made with a spatial resolution high enough to resolve most of the modes to which the measurements are sensitive.

V CONCLUSION

The result of our investigation offers hope that high-resolution observations of oscillations of the solar limb might provide valuable information about low-order p modes of low and intermediate degree. In particular, groups of relatively few modes with $\ell - m \ll \ell$ can be separated from the signal, and the group of sectoral modes ($\ell = m$) can be extracted quite cleanly. Modes with low m, but degree ℓ close or equal to the natural or instrumental cutoff ℓ_m can also be isolated from the others.

Our method is also suitable for identifying internal gravity modes. High-degree g modes trapped in the radiative interior are unlikely to confuse the signal, because their amplitudes should be negligible. Indeed, for g modes we expect a natural cutoff in ℓ due to the high impedance of the convection zone to high-degree modes (Dziembowski and Pamjatnykh 1978, Christensen-Dalsgaard et al. 1980). Atmospheric g modes are distinguishable by their different dispersion relation, and in any case it is unlikely that they enjoy the high coherence of the other modes. Consequently they could be filtered out in a temporal power spectrum.. Therefore the method we propose

should certainly be useful for identifying all observable coherent modes with frequencies below about 1 mHz.

We have not made a careful study of the effect of noise in the data. It would be instructive to create artificial data with noise and then try to recover the modes from which the data were constructed.

Though individual modes cannot be completely isolated in a set of measurements at a single instant of time, the temporal information can often be used to permit unambiguous identification. For example, if we assume a constant rotational splitting of 0.45 μHz, only the retrograde $p_1(\ell = 20)$ and the prograde $f(\ell = 50)$ sectoral modes of even degree (computed from Model 1 of Christensen-Dalsgaard 1982) have frequencies within 5 μHz of 0.750 mHz. Therefore in principle there can be no ambiguity in identifying $p_1(\ell = 20)$ using the combination of data that produced Figure 5 a. Moreover, the prograde $p_1(\ell = 30, m = 14)$ is the only mode in Figure 5d with W_k^2 greater than 20 per cent of $W_{k_c}^2$ and whose frequency is within 5 μHz of 0.900 mHz. These examples typify the situation for low-order p modes, and show that spatial and temporal limb information can be combined to identify p modes of low order.

ACKNOWLEDGEMENTS

DOG is grateful to J-P Zahn for the hospitality of the Observatoires du Pic-du-Midi et de Toulouse, and JL to the CNRS of France for a grant to visit the Institute of Astronomy in Cambridge. The work was supported in part by NASA grants NSG-7511 and NAGW-91. The Joint Institute for Laboratory Astrophysics is supported jointly by the University of Colorado and the National Bureau of Standards of the USA.

REFERENCES

Backus, G. and Gilbert, F., 1970, Phil. Trans., A266, 123-192

Bos, R.J. and Hill, H.A., 1983, Solar Phys., 82, 89-102

Christensen-Dalsgaard, J., 1982, Mon.Not.R.astr.Soc., 199, 735-761

Christensen-Dalsgaard, J., 1984, Proc. Workshop on "Solar seismology" from space (ed. R.K. Ulrich, NASA, Washington D.C.) in press

Christensen-Dalsgaard, J. and Gough, D.O., 1982, Mon.Not.R.astr.Soc., 198, 141-171

Christensen-Dalsgaard, J., Dziembowski, W.A. and Gough, D.O., 1980, Nonradial and nonlinear stellar pulsation (ed. H.A. Hill and W.A. Dziembowski; Springer, Heidelberg) 313-341

Dziembowski, W.A. and Pamjatnykh, A.A., 1978, Pleins feux sur la physique solaire (ed. J. Rösch, CNRS, Paris) 135-40

Hill, H.A., 1978, in The new solar physics, (AAAS Selected symposium 17, ed. J.A. Eddy, Westview, Boulder) 135-214

Rösch, J. and Yerle, R., 1983, Solar Phys., 82, 139-150

Stebbins, R.T., 1984, Mem. Soc. astr. Italiana, in press